Published in final edited form as:
Cancer Gene Ther. 2006 January 1; 13(1): 53–64.

Minimally-Invasive Localization of Oncolytic Herpes Simplex Viral Therapy of Metastatic Pleural Cancer

Brendon M. Stiles, MD[*], **Prasad S. Adusumilli, MD**[*], **Amit Bhargava, MD**[*], **Stephen F. Stanziale, MD**[*], **Teresa H. Kim, MD**[*], **Mei-Ki Chan, BS**[*], **Rumana Huq, MS**[+], **Richard Wong, MD**[*], **Valerie W. Rusch, MD**[*], and **Yuman Fong, MD**[*]

* *From the Department of Surgery and Molecular cytology core facility,*

\+ *Memorial Sloan–Kettering Cancer Center, New York, New York*

Abstract

Purpose—Herpes simplex virus-one (HSV-1) oncolytic therapy and gene therapy are promising treatment modalities against cancer. NV1066, one such HSV-1 virus carries a marker gene for enhanced green fluorescent protein (EGFP). The purpose of this study was to determine whether NV1066 is cytotoxic to lung cancer and whether EGFP is a detectable marker of viral infection *in vitro* and *in vivo*. We further investigated whether EGFP expression in infected cells can be used to localize the virus and to identify small metastatic tumor foci (< 1 mm.) *in vivo* by means of minimally invasive endoscopic systems equipped with fluorescent filters.

Experimental Design—In A549 human lung cancer cells, *in vitro* viral replication was determined by plaque assay, cell kill by LDH release assay, and EGFP expression by flow cytometry. *In vivo*, A549 cells were injected into the pleural cavity of athymic mice. Mice were treated with intrapleural injection of NV1066 or saline and examined for EGFP expression in tumor deposits using a stereomicroscope or a fluorescent thoracoscopic system.

Results—NV1066 replicated in, expressed EGFP in infected cells and killed tumor cells *in vitro*. *In vivo*, treatment with intrapleural NV1066 decreased pleural disease burden, as measured by chest wall nodule counts and organ weights. EGFP was easily visualized in tumor deposits, including microscopic foci, by fluorescent thoracoscopy.

Conclusions—NV1066 has significant oncolytic activity against a human NSCLC cell line and is effective in limiting the progression of metastatic disease in an *in vivo* orthotopic model. By incorporating fluorescent filters into endoscopic systems, a minimally-invasive means for diagnosing small metastatic pleural deposits and localization of viral therapy for thoracic malignancies may be developed using the EGFP marker gene inserted in oncolytic herpes simplex viruses.

Keywords

Gene therapy; Green fluorescent protein; Lung neoplasm; Minimally-invasive; Targeted therapy; Thoracoscopy; Bronchoscopy

Address for correspondence: Yuman Fong, MD, Department of Surgery, H1223, Memorial Sloan-Kettering Cancer Center, 1275 York Avenue, New York, New York 10021, Phone: (212) 639-2016 Fax: (212) 639-4031, E-mail:fongy@mskcc.org.

Supported in part by training grant T32 CA09501 (B.M.S.), AACR-AstraZeneca Cancer Research and Prevention Foundation Fellowship (P.S.A), grants RO1 CA 76416 and RO1 CA/DK80982 (Y.F.) from the National Institutes of Health, grant MBC-99366 (Y.F.) from the American Cancer Society, grant BC024118 from the US Army (Y.F.), grant IMG0402501 from the Susan Komen Cancer foundation (Y.F. and P.S.A.) and grant 032047 from Flight Attendant Medical Research Institute (Y.F. and P.S.A.)

Study presented at the 6th annual meeting of 'American Society of Gene Therapy', 2003 in Washington DC.

Abbreviations

CMV: cytomegalovirus; EGFP: enhanced green fluorescent protein; HSV-1: herpes simplex virus-1; LDH: lactate dehydrogenase; MIS: minimally-invasive surgical

INTRODUCTION

Lung cancer is the leading cause of cancer deaths in the United States(1). Eighty-six percent of patients diagnosed with lung cancer die within 5 years(2). Herpes simplex virus mediated oncolysis and gene therapy have emerged as promising treatment modalities against cancer (3–10). Oncolysis results from the replicative life cycle of the virus, which lyses infected cells for release of viral progeny. Given the specificity of herpes viral replication for tumor cells, we sought to determine whether NV1066, a HSV-1 mutant virus is cytotoxic to a human non-small cell lung cancer (NSCLC) cell line, both *in vitro* and *in vivo* in a murine xenograft pleural tumor model. Furthermore, even patients diagnosed as early stage lung cancer by conventional pathologic criteria have been found to have a significant incidence of metastatic disease, both in the pleural cavity and in the lymph nodes(11). Such foci of disease are extremely difficult to diagnose preoperatively. Metastatic disease in the pleural cavity may indicate a more aggressive tumor biology an a higher risk of recurrence(12–16), which could contribute to the decreased survival often seen in these patients. As such, new techniques are needed to both diagnose and treat metastatic pleural spread of NSCLC. Viral-based gene therapy makes use of the ability of herpes viral mutants to selectively replicate within tumor cells, for targeted transgene expression(17). NV1066 used in this study is genetically engineered to express enhanced green fluorescent protein (EGFP) in the infected cells(18). Previous studies from our laboratory have shown that NV1066-induced EGFP expression can be used as a marker of viral infection, and thus to identify cancer(19;20). In this study we further seek to determine whether NV1066-induced EGFP expression can be used to diagnose small metastatic deposits of pleural cancer invisible to the naked eye in an *in vivo* pleural model and the sensitivity of such detection method.

Targeted therapy by oncolytic viruses differ from conventional chemotherapeutic agents in that a very low dose of virus can be administered to initially infect only a small proportion of cancer cells. These viruses subsequently replicate and propagate upon lyses of the infected cell to infect neighboring cancer cells. While techniques for assessing viral infection and spread in cell culture or animal models are readily available, safe, minimally-invasive methods for detecting regional distribution and activity in man are needed to facilitate clinical use of these viruses. Current methods necessitate tissue biopsies to determine viral presence in specimens using histological or PCR-based techniques(7;21;22). In this study, we investigated the reliability of NV1066-induced EGFP expression as a marker of viral infection and spread both *in vitro* and *in vivo* and whether viral therapy could be followed by a minimally-invasive technique. Fluorescent proteins such as EGFP are well suited as markers for viral therapy. EGFP is a stable protein that does not require additional substrates or co-factors for its expression(23). While EGFP and its derivative proteins have been extensively used as reporters and / or markers in numerous biological studies, their use as a tumor-specific localization marker and as a marker of oncolytic viral therapy as reported in this study is an emerging technology(24;25). While the studies are conducted in mice, it is envisioned that such optical imaging for human application is cost-effective, rapid, easy to use, and can be readily applied *in vivo* by incorporating fluorescent filters in endoscopic systems.

MATERIALS AND METHODS

Cells and Virus

A549 human NSCLC purchased from the ATCC (Rockville, MD) were used for experiments. Cells were grown in Ham's F-12 media with 10% FCS, 100 U/ml penicillin, and 100 mg/ml streptomycin. NV1066 is a replication-competent, attenuated herpes simplex-1 mutant virus described in detail previously(26). A sequence containing the gene for enhanced green fluorescent protein (EGFP) under the control of a constitutive cytomegalovirus (CMV) promoter was inserted into the internal repeat sequence of the parent virus. This resulted in loss of single copies of the viral genes, ICP-4, ICP-0, and $\gamma_1$34.5. These deletions increase the tumor specificity of viral replication and also serve to attenuate the potential neurovirulence of the parent strain. Viral stocks were propagated on Vero cells, harvested by freeze-thaw lysis and sonication, and titered by standard plaque assay.

Cytotoxicity assay and viral titering

A549 cells were plated in 12 well flat-bottom plates (Costar, Corning Inc., Corning, NY) in 1 ml of media and subsequently infected with NV1066 at multiplicities of infection (MOI: number of viral plaque forming units per tumor cell) of 0.1 or 1.0, in a total volume of 50 μl of saline. Every other day after infection, media was removed; cells were washed with PBS, and lysed (1.35% Triton-X solution) to release intracellular lactate dehydrogenase (LDH). LDH was quantified using a Cytotox 96 nonradioactive cytotoxicity assay (Promega, Madison, WI) that measures the conversion of a tetrazolium salt into a red formazan product. The amount of color formed is directly proportional to the number of lysed cells. Absorbance was measured at 450 nm using a microplate reader (EL 312e: Bio-Tek Instruments, Winooski VT.) Results are expressed as surviving fraction, based on the measured absorbance of treated cellular lysates, compared to that of untreated, control cellular lysates. All samples were tested in triplicate. Experiments were repeated at least twice to ensure reproducibility. To determine release of viral progeny from cells, media was collected on days 3–8 after infection from sample wells infected with NV1066 at MOIs of 0.1 and 1.0, prepared as in the cytotoxicity assay. Serial dilutions were made of the suspension and used to infect confluent Vero cells in a standard viral plaque assay. Plaques are fixed in agar, grown for 48 hours, and counted after staining with a neutral red solution.

Flow cytometry for EGFP

A549 cells were plated in 6 well plates with 2 ml of media and subsequently infected with NV1066 at MOIs of 0.1 or 1.0 in 100 μl of PBS. Untreated cells served as negative controls. Cells were harvested with 0.25% trypsin in 0.02% EDTA, combined with the supernatant fraction, centrifuged, washed in PBS, and brought up in 100 μl of PBS. Five μl of 7-amino-actinomycin (7-AAD, BD Pharmingen, San Diego, CA) was added as an exclusion dye for cell viability. Data for EGFP expression from 10^4 cells was acquired on a FACS Calibur machine equipped with Cell Quest software (Becton Dickinson, San Jose, CA). Results are reported as percent of live cells expressing EGFP.

Fluorimetry for EGFP

A549 cells were plated in a T-75 flask and subsequently infected with NV1066 or mock infected with PBS. When 95% or greater of the infected cell population demonstrated EGFP expression by flow cytometry (as described above), cells were harvested with 0.25% trypsin in 0.02% EDTA and serially diluted between 1 x 10^7 and 1 x 10^4 cells in 100 μl of PBS. Cell suspensions of both infected and control cells were plated in quadruplicate on 96-well white fluorimeter plates and read on a Fluoroskan Ascent FL fluorimeter (Thermo Electron Corporation, Vantaa, Finland) at an excitation wavelength of 475 nm and an emission wavelength of 510 nm, taking

the average of 6 readings per well. Results are reported as fluorescent intensity (RFU) per well and as a ratio of RFU of infected cells to noninfected cells.

Animal experiments

Animal procedures were approved by the Memorial Sloan-Kettering Institutional Animal Care and Use Committee (New York, NY). Six-week-old male athymic mice (National Cancer Institute, Bethesda, MD) used for experiments were provided food and water ad libitum. Prior to experiments, anesthesia was induced by means of a single intraperitoneal injection of a ketamine/xylazine mixture in sterile water.

EGFP expression over time—To establish flank tumors, 2×10^6 A549 cells were harvested and resuspended (50% PBS, 50% Matrigel, BD Biosciences, Bedford, MA) in a total of 50 μl. Mice were anesthetized by intraperitoneal injection of ketamine and xylazine in sterile water. The cell suspension was injected into the flanks of mice using a 28 gauge needle. Tumors were measured in two dimensions with Vernier calipers and volume determined using the formula for a prolate spheroid, $4/3(\pi)ab^2$, with "a" as the radius of the long axis and "b" the radius of the short axis in millimeters. Tumors were followed by weekly volume determination until they had reached an average volume of 100 mm^3. To determine EGFP expression following viral treatment, 1×10^6 pfu of NV1066 (in 25 μl of PBS) was administered by direct intratumoral injection. Tumors were harvested at 24, 48, and 96 hours time points and homogenized in 4 ml/g tissue of Passive Lysis Buffer (Promega, Madison, WI). Samples underwent 3 cycles of freeze-thaw lysis, followed by centrifugation at 14,000 rpm for 15 minutes. Fluorescent activity was assessed by fluorimetry using 100 μl of supernatant from each sample, with excitation and emission parameters as described for the *in vitro* studies. Results are reported as RFU / mg total protein.

Metastatic pleural carcinomatosis—One $\times 10^6$ A549 cells were injected percutaneously into the pleural cavity of athymic mice in 100 μl of PBS as described previously. On the day following tumor cell injection, mice were divided into 2 groups and then treated, again by percutaneous injection into the pleural cavity with either 50 μl of PBS containing 1×10^7 pfu of NV1066 (n=9) or with 50 μl of PBS alone (n=5). Three weeks after tumor inoculation, animals were sacrificed and the heart, lungs, and mediastinum were harvested en bloc and weighed. Organ weights taken from same-age, non-tumor bearing animals (n=4) were also obtained. For both PBS and NV1066 treated groups of animals, chest wall nodules were counted after removal of organs as a measure of treatment effect on pleural carcinomatosis.

In vivo imaging—Two $\times 10^6$ A549 cells were injected into the pleural cavities of mice as described previously. Animals (n=4) were treated with 1×10^7 pfu of intrapleural NV1066 as above at separate time points. For imaging of metastatic disease, mice were treated day 2 after cell injection. For imaging of gross pleural disease, mice were treated 3 weeks after cell injection. Mice were examined 48 hours later in both cases, using a fluorescent thoracoscopic system and by fluorescent stereomicroscopy. The thoracoscopic system was developed in concert with Olympus America, Inc. (Scientific Equipment Division, Melville, NY) to allow for the detection of EGFP as well as routine white light. The light source was an Olympus Visera CLV-U40 model with an adaptable excitation filter set at 470 ± 20 nm. The camera processor was an Olympus Visera OTV-S7V with an emission filter set at 510 nm. Imaging was performed in both brightfield and fluorescent modes. With the stereomicroscope (Olympus America Inc., Melville, NY), imaging was also performed in brightfield mode and after placement of both excitation and emission filters to detect EGFP. The excitation filter was fixed passage 470 ± 40 nm wavelength light as GFP has a minor excitation peak at 475 nm. The emission filter was fixed at 500 nm, to accommodate the emission peak of GFP at 509 nm. The image-capture system consisted of a Retiga EX digital CCD camera (Qimaging, Burnaby,

BC). For generation of topography maps, images were presented in Zeiss LSM510 software (v3.2) using the "pseudo 3D" tool. Individual pixel intensity values of the image are mapped upon a height grid to quantify fluorescent intensity. Pixels of high intensity are represented by the grid peaks, while pixels of low intensity are represented by grid valleys.

Viral specificity for tumor

Samples of tissue emitting EGFP under stereomicroscopy were frozen in Tissue-Tek embedding medium (Sakura Finetek, Torrance, CA) and sectioned by cryotome for histological examination. Following paraformaldehyde fixation, slides were first examined under fluorescent microscopy for EGFP expression, then stained with hematoxylin and eosin (H & E) to determine whether EGFP expression localized to foci of cancer. To confirm that EGFP expression was localizing virus, serial sections that expressed EGFP were stained with rabbit polyclonal HSV-1 antibody using a Histomouse-SP Bulk Staining Kit (Zymed laboratories Inc., San Francisco, CA) and compared for EGFP expression and viral antibody binding. An institutional animal pathologist confirmed all results.

RESULTS

Cytotoxicity assay and viral titering

NV1066 progressively killed A549 cells *in vitro* at both MOIs (Figure 1A). Although cell kill was initially more pronounced at the higher MOI of 1.0, an MOI of 0.1 also demonstrated significant cytotoxic effects over time. By day 9, *in vitro* cell kill at MOIs of 0.1 and 1.0 is 83 ± 2.4% and 96 ± 0.4% respectively ($p < .01$, t-test). Significant *in vitro* viral replication occurred in A549 cells following infection at MOIs of 0.1 and 1.0 (Figure 1B*)*. Viral titers increase steadily following infection, then subsequently decline as fewer live cells remain to support further replication. Treatment of the cells with the lower MOI led to higher peak viral titers as determined by viral plaque assay, 5.3×10^6 pfu/ml vs. 2.6×10^6 pfu/ml ($p < .001$, t-test). This phenomenon often occurs following *in vitro* treatment with oncolytic HSV-1 mutants, as early cytotoxic death in cell populations treated with the higher MOI limits the cell number and time for productive cellular replication of virus. Peak viral titers at the lower MOI represent an approximate 5300-fold increase over the initial dose of virus.

Flow cytometry for EGFP

The EGFP transgene carried by NV1066 was used as a marker of viral infection in A549 cells. This technique has been used previously to assess transduction efficiency of HSV-1 based amplicon vectors(27). EGFP expression was determined by FACS analysis. Control populations of cells did not express EGFP (Figure 2A). In contrast, over 60% of cells infected with NV1066 at an MOI of 1.0 expressed EGFP after 48 hours (Figure 2B). EGFP expression in A549 cell populations was initially dose-dependent after treatment at MOIs of 0.1 and 1.0 (Figure 2C). Following viral replication, EGFP expression in live cells increased over time to nearly 100% at both MOIs ($p < .001$ vs. untreated control cells, t-test).

Fluorimetry for EGFP

In order to establish the cell number needed to differentiate infected from uninfected cells by standard fluorescence detection, fluorimetry was performed on populations of cells. Significant differences in fluorescent intensity were found with as few as 1000 cells ($p < .005$, t-test). The fluorescent signal from NV1066 infected cells increased linearly with infected cell number (not shown). By comparing the RFU of equal numbers of infected cells to uninfected tumor cells, a fluorescence intensity ratio could be calculated (Figure 3A). Ratios that have been previously demonstrated to allow for clinical detection of tumors using minimally-invasive techniques were obtained *in vitro* at approximately 1×10^4 infected cells. At that number of

cells, measured fluorescent intensity was 3.4-fold (± 0.1) higher in cells infected with NV1066 than in control cells. Ratios increased progressively with higher numbers of infected cells.

Time course of *in vivo* EGFP expression

A previous study from our laboratory has demonstrated the ability of NV1066 to replicate *in vivo* in murine flank tumors(28). Viral titers increase over time as measured by real-time PCR for viral genomic DNA, with a large replication burst evident between 24–48 hours. In the present study, we assessed virus-induced EGFP expression over time, as measured by fluorimetry of protein extracts from tumors. At 24 hours following infection, EGFP expression (RFU / mg tissue) in NV1066 infected tumors was higher than in control tumors, although the difference was not statistically significant (Figure 3B, $p = 0.2$). By 48 hours however, EGFP expression in infected tumors was significantly higher than in control tumors, 4.3×10^5 vs. 1.2×10^5 RFU / mg, a 3.6-fold increase in fluorescent intensity ($p = .04$, t-test). Fluorescence increased to 7.1×10^5 RFU / mg by 96 hours following infection, a 5.9-fold increase over control ($p = .02$, t-test). We therefore decided to use time points of 48 hours or later to assess for EGFP expression in the pleural tumor model, as these time points were more likely to allow for virus detection.

Treatment of *in vivo* tumors

Direct injection of NV1066 significantly suppressed growth of pleural A549 tumors. Organ and tumor weights of PBS treated, NV1066 treated, and matched control animals were 536 (±70) mg, 351 (±38) mg, and 373 (±24) mg respectively. There was no statistically significant difference between NV1066 treated and matched control animal organ weights, while the PBS treated animals had significantly higher organ weights, reflecting increased tumor burden ($p < .01$, vs. NV1066 treated animals, t-test). Similarly, PBS treated animals had an average of 71 ± 7 chest wall nodules compared to only 7.7 ± 7.5 nodules in the NV1066 treated group (Figure 4A). Seven out of 9 animals in the NV1066 treated group had no evidence of macroscopic chest wall nodules or other tumor burden, compared to 0 of 5 mice in the PBS group. Representative photographs of the chest wall of a control mouse (Figure 4B) and of a mouse treated with NV1066 (Figure 4C) are shown.

In vivo imaging

Following administration of NV1066 *in vivo*, EGFP expression was easily visualized by fluorescent microscopy in the pleural tumor model. EGFP expression was visualized in all NV1066 treated animals and localized to tumor deposits, sparing normal tissues. Green fluorescence could be used to identify tumor deposits, localizing even microscopic collections of tumor cells not apparent under brightfield microscopy. Similarly, using the fluorescent thoracoscopic system, EGFP expression also localized tumor foci. The pleural cavity was examined in both white light and GFP modes. The thoracoscopic device can be easily changed between the two modes without pausing the procedure. Figures 5A-D demonstrates images obtained using the thoracoscopic system. Non-tumor bearing thoracic organs did not fluoresce strongly *in vivo* when examined through the EGFP filter and were easily distinguished from infected tumor deposits. Of note, microscopic tumor deposits not identified on brightfield microscopy or thoracoscopy could be identified in the fluorescent modes of each. Expression of EGFP on the lung or chest wall (Figure 6A-B) identified tumor deposits that would otherwise have been missed with standard imaging. Presence of tumor cells was confirmed by histology. Using computer software, topography maps of EGFP expression could be generated from the digital images obtained with the fluorescent microscopic or thoracoscopic systems (Figure 6C). The x and y axis represent a biplanar digital image of the chest wall. The z-axis represents the fluorescent intensity detected. This technology enables quantification of *in vivo* fluorescent intensity.

Viral specificity for tumor

Following pleural administration of NV1066, strong EGFP expression was noted in tumor nodules when examining serial pathological sections. Some autofluorescence was apparent in the bronchial system, but this was easily distinguished from virus-induced EGFP expression. All sections that expressed EGFP were found to have tumor cell infiltrates corresponding to areas of expression. Representative sections of a nodule expressing EGFP taken from the surface of the pleura are shown in Figures 7A–C. H&E staining confirmed that EGFP expression localized to foci of cancer (Figure 7B). Staining for polyclonal HSV-1 antibody corresponded to areas of EGFP expression by histology (Figure 7C). No viral staining was evident in tissues that did not express EGFP in all samples sectioned.

DISCUSSION

Viruses are being tested as oncolytic agents that selectively undergo lytic replication in tumor cells. DNA viruses are obligate intracellular parasites whose lytic cycle is totally dependent on their ability to commandeer the replicative machinery of their host. Thus, like tumor cells DNA tumor viruses evolved mechanisms that uncouple cellular replication from the many intracellular and extracellular factors that normally control it so tightly. A profound functional overlap exists between DNA viruses and tumor cells with respect to the cellular checkpoints they must perturb to ensure their replication. This common ground forms the basis for several oncolytic viral therapies(29). Oncolytic HSV-1 mutants are replication-competent viruses that selectively infect and lyse tumor cells, while sparing normal tissues. HSV-1 mutants have been demonstrated to be effective against a number of malignancies in experimental models(30–37). Three such viruses are currently in clinical trials for recurrent malignant gliomas and for unresectable colorectal metastases to the liver (7,8,38). We have previously demonstrated the efficacy of a herpes viral mutant, NV1020, in the treatment of pleural tumors in animal models (39). In this study, we used NV1066, another multi-mutated, replication-competent oncolytic HSV-1 virus, which carries a transgene for the marker protein, EGFP. Cells were demonstrated to support viral replication, with up to 5300-fold increases in viral titers *in vitro*. Viral titers peaked from day 4 to 6, because of low plating confluence at the beginning of the experiment. Over the period of time, virus was able to replicate, propagate, infect and lyse most of the cells by day 7 representing *in vivo* spread. *In vitro*, initial doses of NV1066 as low as one viral plaque forming unit per 10 tumor cells killed over 80% of A549 cell populations after one week in culture. The efficacy of NV1066 was also apparent *in vivo* in mouse xenograft models, in the treatment of metastatic pleural disease. NV1066 decreased progression of tumor burden in the pleural cavity. A single dose of virus led to an 89% reduction in chest wall nodule development. Seven of nine animals in the NV1066 treated groups were free of macroscopic disease at the time of sacrifice, compared to none in the PBS group.

Spread of malignancies to the pleural cavity, resulting in malignant pleural effusions and pleural metastatic disease are associated with a dismal prognosis, with most patients surviving only a few months after the diagnosis is made(40–47). While NSCLC is the most common cause of malignant disease of the pleura, the pleural model used in this study is also relevant to other cancer types, including mesothelioma, breast, ovarian, and lymphoid cancers(48–50). Pleural spread of NSCLC is thought to result from either exfoliation and/or lymphatic spread. Such spread, diagnosed by conventional imaging studies, video assisted thoracic surgery (VATS), or pleural lavage cytology (PLC) is associated with an increased rate of tumor recurrence and with the development of carcinomatous pleuritis (malignant pleural effusion, disseminated pleural tumors, or both). A prospective trial of intraoperative, intrapleural chemotherapy reduced postoperative carcinomatous pleuritis in patients with metastatic pleural disease(51). Intrapleural therapy with NV1066 could have a similar treatment effect as demonstrated in this study, potentially improving survival in this subgroup of patients.

When administering HSV-1 mutants and other oncolytic viruses or viral vectors clinically, assessing viral infection and spread *in vivo* may be somewhat cumbersome. Current trials rely on tissue biopsies followed by immunocytochemistry or PCR-based techniques, requiring samples of normal tissues as well as of the targeted tumors. Attempts have been made to follow viral therapy by non-invasive methods in several preclinical studies. The activity of *in vivo* reporter genes can be assessed radiographically using radiolabeled ligands, antigens, or substrates(52–55). More recently, positron emission tomography (PET) reporter transgenes have been developed(56–58). Such imaging strategies have limitations similar to conventional radiological techniques and may only detect areas with large amounts of viral uptake. As more replication-competent viruses and viral vectors progress toward clinical use, more accurate techniques to rapidly assess viral infection and spread *in vivo* are needed. Minimally-invasive techniques are a potentially attractive method for following *in vivo* viral distribution, as their sensitivity and specificity are likely higher than currently available noninvasive techniques (59). Importantly, minimally-invasive techniques also allow for the possibility of tissue sampling should the need arise, whereas noninvasive imaging procedures do not. With an appropriate marker gene and detection system, a wide variety of minimally-invasive endoscopic procedures could be utilized to assess viral distribution in numerous body cavities, including laryngoscopy, bronchoscopy, mediastinoscopy, upper and lower gastrointestinal endoscopy, thoracoscopy, laparoscopy, cystoscopy, and arthroscopy.

Genetically engineered herpes viruses may be useful in the treatment of cancer based upon their oncolytic properties alone, or as vectors to carry therapeutic or immunomodulatory transgenes to targeted tumors. NV1066 carries such a marker gene, a constitutively expressed transgene for EGFP, the protein product of which is identifiable 4–6 hours following viral entry into cells. While green fluorescent protein and its derivative proteins have been used extensively as reporters and/or markers in numerous biologic studies(60–65), their use to determine infection and spread of replication-competent viral vectors *in vivo* is an emerging technology. Previous studies have demonstrated that the fluorescent signal from cells constitutively expressing GFP correlates strongly with cell number in vitro(66). In this study, using a combination of flow cytometry and fluorimetry on populations of cells infected with NV1066, we demonstrate that the fluorescent signal correlates with the number of cells infected with our virus *in vitro*. This principle was extended to *in vivo* studies. In a murine flank tumor model, fluorescence increased over time with viral replication so that infected tumors were clearly distinguishable from non-infected tumors by 48 hours after infection. Furthermore, following intrapleural administration of NV1066, *in situ* metastatic tumor deposits could be distinguished by green fluorescence using fluorescent stereomicroscopy or a thoracoscopic system with appropriate fluorescent filters. Samples of tissue expressing EGFP were harvested, sectioned serially, and examined for the presence of virus. All tissue that expressed EGFP was noted to stain positively for HSV-1 polyclonal antibody, while no viral staining was evident in tissues not expressing EGFP. This suggests that fluorescent protein expression can be used as a surrogate to identify viral distribution *in vivo* without the need for extensive tissue sampling.

Fluorescent endoscopic, laparoscopic, and thoracoscopic techniques have previously been reported to enhance tumor visualization. Using the exogenously administered photosensitizer, 5-aminolevulinic acid (ALA), laparoscopic visualization of peritoneal tumor deposits in an animal model was improved by 17–35%, and that of pleural nodules by 30% (67)compared to conventional white-light laparoscopy alone(68–70). ALA requires endogenous metabolism before it can fluoresce. Although it specifically accumulates in tumor cells, its use is limited by a narrow time window for visualization and by the possibility of skin phototoxicity. Tumor specific expression of EGFP produced by viral infection has a similar potential to improve detection of thoracic tumor deposits using fluorescent thoracoscopy, bronchoscopy, and mediastinoscopy in addition to being therapeutic without added toxicity.

Previous studies have found GFP expression in transfected tumor cells to allow for detection of metastases down to the single-cell level in exposed or fresh isolated organs or tissues(71). In subsequent studies, fluorescent localization was found to be more rapid and sensitive than histopathology or immunohistochemistry for identifying tumor deposits(72–74). Furthermore, fluorescent intensity of GFP-expressing tumors has been suggested to be a more accurate measure of biomass than tumor volume measurements(75). While those studies relied upon stably transfected GFP-expressing cells, we report here a method for identifying tumor cells *in vivo* with a therapeutic viral vector, a model that may be more readily applied clinically. Current imaging techniques including computed tomography, magnetic resonance imaging, and PET generally cannot detect tumor foci whose diameter is smaller than 3–5 mm, or about $10^7 – 10^8$ cells(76;77). In our current study, using a minimally-invasive thoracoscopic procedure, green fluorescence could be used to detect even small metastatic tumor deposits invisible to the naked eye. Clinically, the fluorescence ratio between tumor and surrounding normal tissue determines the ability to distinguish the two by optical contrast. Previous studies using fluorescent diagnosis techniques have indicated that fluorescent intensity ratios of three or greater are sufficient to distinguish between induced fluorescence in tumors and autofluorescence in normal tissues(78). Our *in vitro* studies suggest that such ratios may be achieved with as few as 1×10^4 tumor cells infected with NV1066, a 3–4 log improvement over the lower limits of radiological detection. Earlier detection and treatment of pleural spread of NSCLC may potentially improve disease-free and overall survival in this group of patients. In addition to pleural tumor model, which resembles superficial cancer, NV1066-induced EGFP expression was also found to be useful in detecting metastasis even when embedded inside the solid organs in mouse (data not shown). EGFP expression in a particular cell or cancer tissue is dependent upon the cellular proliferation, i.e. aggressiveness of the cancer. EGFP expression was noted with NV1066 doses as low as 2×10^4 pfu in identifying intracavitary tumors.

In conclusion, NV1066 has significant oncolytic activity against a human NSCLC cell line and is effective in limiting the progression of metastatic disease in an *in vivo* orthotopic model. Expression of EGFP in infected cells can be used to localize the virus and helps to localize even small metastatic tumor deposits *in vivo* by minimally-invasive means. By capturing and reconstructing digital images, EGFP expression *in vivo* can be detected in a semi-quantitive manner. We hope to incorporate this technology into our next generation of thoracoscopes, laparoscopes, and other endoscopes to allow for real-time spectral analysis of fluorescent intensities and to correlate this with viral and tumor load. Potential analytical applications include monitoring dissemination of and treatment response to viral therapy, aid in diagnosis and staging of malignancies, and aid in determining the appropriateness of surgery and/or neoadjuvant or adjuvant therapy. The technique reported here can be applied clinically in any oncolytic viral or viral-based gene therapy trials to monitor viral distribution and activity *in vivo* by minimally-invasive means.

Acknowledgements

The authors thank Brian Horsburgh, Ph.D. and Medigene, Inc. for constructing and providing us with the NV1066 virus. We thank Mithat Gonen, Ph.D., of the Department of Epidemiology and Biostatistics, and Katia Manova, Ph.D., John Waka, B.S., and members of the Molecular Cytology Core Facility at Memorial Sloan-Kettering Cancer Center for their assistance with this project. We thank Hai Nguyen, V.M.D., of the Research Animal Resource Center of Cornell University Medical College for review of pathology specimens. Special thanks to Kan Matsumoto from Olympus America Inc., for design and construction of the fluorescent thoracoscopic system.

References

1. 2004 Cancer Facts & Figures. Available at: http://www.cancer.org/downloads/STT?CAFF_finalPWSecured.pdf Accessed July 1st, 2004.

2. Carney DN. Lung cancer--time to move on from chemotherapy. N Engl J Med 2002;346(2):126–128. [PubMed: 11784881]
3. Roizman B. The function of herpes simplex virus genes: a primer for genetic engineering of novel vectors. Proc Natl Acad Sci U S A 1996;93(21):11307–11312. [PubMed: 8876131]
4. Stiles BM, Bhargava A, Adusumilli PS, Stanziale SF, Kim TH, Rusch VW, et al. The replication-competent oncolytic herpes simplex mutant virus NV1066 is effective in the treatment of esophageal cancer. Surgery 2003;134(2):357–364. [PubMed: 12947341]
5. Bennett JJ, Adusumilli P, Petrowsky H, Burt BM, Roberts G, Delman KA, et al. Up-regulation of GADD34 mediates the synergistic anticancer activity of mitomycin C and a gamma134.5 deleted oncolytic herpes virus (G207). FASEB J 2004;18(9):1001–1003. [PubMed: 15059970]
6. Carew JF, Kooby DA, Halterman MW, Federoff HJ, Fong Y. Selective infection and cytolysis of human head and neck squamous cell carcinoma with sparing of normal mucosa by a cytotoxic herpes simplex virus type 1 (G207). Hum Gene Ther 1999;10(10):1599–1606. [PubMed: 10428205]
7. Fong Y, Kemeny N, Jarnagin S, Stanziale S, Guilfoyle B, Gusani N et al. Phase 1 study of a replication-competent Herpes Simplex oncolytic virus for treatment of hepatic colorectal metastases. Abstract # 27, 2002 American Society of Clinical Oncology 38th annual meeting proceedings Vol 2:Part1, 8a.
8. Markert JM, Medlock MD, Rabkin SD, Gillespie GY, Todo T, Hunter WD, et al. Conditionally replicating herpes simplex virus mutant, G207 for the treatment of malignant glioma: results of a phase I trial. Gene Ther 2000;7(10):867–874. [PubMed: 10845725]
9. Mineta T, Rabkin SD, Yazaki T, Hunter WD, Martuza RL. Attenuated multi-mutated herpes simplex virus-1 for the treatment of malignant gliomas. Nat Med 1995;1(9):938–943. [PubMed: 7585221]
10. Rampling R, Cruickshank G, Papanastassiou V, Nicoll J, Hadley D, Brennan D, et al. Toxicity evaluation of replication-competent herpes simplex virus (ICP 34.5 null mutant 1716) in patients with recurrent malignant glioma. Gene Ther 2000;7(10):859–866. [PubMed: 10845724]
11. Jiao X, Krasna MJ. Clinical significance of micrometastasis in lung and esophageal cancer: a new paradigm in thoracic oncology. Ann Thorac Surg 2002;74(1):278–284. [PubMed: 12118789]
12. Buhr J, Berghauser KH, Gonner S, Kelm C, Burkhardt EA, Padberg WM. The prognostic significance of tumor cell detection in intraoperative pleural lavage and lung tissue cultures for patients with lung cancer. J Thorac Cardiovasc Surg 1997;113(4):683–690. [PubMed: 9104977]
13. Dresler CM, Fratelli C, Babb J. Prognostic value of positive pleural lavage in patients with lung cancer resection. Ann Thorac Surg 1999;67(5):1435–1439. [PubMed: 10355426]
14. Higashiyama M, Doi O, Kodama K, Yokouchi H, Tateishi R, Horai T, et al. Pleural lavage cytology immediately after thoracotomy and before closure of the thoracic cavity for lung cancer without pleural effusion and dissemination: clinicopathologic and prognostic analysis. Ann Surg Oncol 1997;4(5):409–415. [PubMed: 9259968]
15. Okumura M, Ohshima S, Kotake Y, Morino H, Kikui M, Yasumitsu T. Intraoperative pleural lavage cytology in lung cancer patients. Ann Thorac Surg 1991;51(4):599–604. [PubMed: 2012419]
16. Kondo H, Asamura H, Suemasu K, Goya T, Tsuchiya R, Naruke T, et al. Prognostic significance of pleural lavage cytology immediately after thoracotomy in patients with lung cancer. J Thorac Cardiovasc Surg 1993;106(6):1092–1097. [PubMed: 8246544]
17. Roizman B. The function of herpes simplex virus genes: a primer for genetic engineering of novel vectors. Proc Natl Acad Sci U S A 1996;93(21):11307–11312. [PubMed: 8876131]
18. Wong RJ, Joe JK, Kim SH, Shah JP, Horsburgh B, Fong Y. Oncolytic herpesvirus effectively treats murine squamous cell carcinoma and spreads by natural lymphatics to treat sites of lymphatic metastases. Hum Gene Ther 2002;13(10):1213–1223. [PubMed: 12133274]
19. Stiles BM, Bhargava A, Adusumilli PS, Stanziale SF, Kim TH, Rusch VW, et al. The replication-competent oncolytic herpes simplex mutant virus NV1066 is effective in the treatment of esophageal cancer. Surgery 2003;134(2):357–364. [PubMed: 12947341]
20. Stanziale SF, Stiles BM, Bhargava A, Kerns SA, Kalakonda N, Fong Y. Oncolytic herpes simplex virus-1 mutant expressing green fluorescent protein can detect and treat peritoneal cancer. Hum Gene Ther 2004;15(6):609–618. [PubMed: 15212719]
21. Rampling R, Cruickshank G, Papanastassiou V, Nicoll J, Hadley D, Brennan D, et al. Toxicity evaluation of replication-competent herpes simplex virus (ICP 34.5 null mutant 1716) in patients with recurrent malignant glioma. Gene Ther 2000;7(10):859–866. [PubMed: 10845724]

22. Markert JM, Medlock MD, Rabkin SD, Gillespie GY, Todo T, Hunter WD, et al. Conditionally replicating herpes simplex virus mutant, G207 for the treatment of malignant glioma: results of a phase I trial. Gene Ther 2000;7(10):867–874. [PubMed: 10845725]
23. Cormack BP, Valdivia RH, Falkow S. FACS-optimized mutants of the green fluorescent protein (GFP). Gene 1996;173(1 Spec):33–38. [PubMed: 8707053]
24. Stiles BM, Bhargava A, Adusumilli PS, Stanziale SF, Kim TH, Rusch VW, et al. The replication-competent oncolytic herpes simplex mutant virus NV1066 is effective in the treatment of esophageal cancer. Surgery 2003;134(2):357–364. [PubMed: 12947341]
25. Stanziale SF, Stiles BM, Bhargava A, Kerns SA, Kalakonda N, Fong Y. Oncolytic herpes simplex virus-1 mutant expressing green fluorescent protein can detect and treat peritoneal cancer. Hum Gene Ther 2004;15(6):609–618. [PubMed: 15212719]
26. Wong RJ, Joe JK, Kim SH, Shah JP, Horsburgh B, Fong Y. Oncolytic herpesvirus effectively treats murine squamous cell carcinoma and spreads by natural lymphatics to treat sites of lymphatic metastases. Hum Gene Ther 2002;13(10):1213–1223. [PubMed: 12133274]
27. Nunez R, Ackermann M, Saeki Y, Chiocca A, Fraefel C. Flow cytometric assessment of transduction efficiency and cytotoxicity of herpes simplex virus type 1-based amplicon vectors. Cytometry 2001;44(2):93–99. [PubMed: 11378858]
28. Stiles BM, Bhargava A, Adusumilli PS, Stanziale SF, Kim TH, Rusch VW, et al. The replication-competent oncolytic herpes simplex mutant virus NV1066 is effective in the treatment of esophageal cancer. Surgery 2003;134(2):357–364. [PubMed: 12947341]
29. O'shea CC. DNA tumor viruses - the spies who lyse us. Curr Opin Genet Dev 2005;15(1):18–26. [PubMed: 15661529]
30. Wong RJ, Joe JK, Kim SH, Shah JP, Horsburgh B, Fong Y. Oncolytic herpesvirus effectively treats murine squamous cell carcinoma and spreads by natural lymphatics to treat sites of lymphatic metastases. Hum Gene Ther 2002;13(10):1213–1223. [PubMed: 12133274]
31. Toda M, Rabkin SD, Martuza RL. Treatment of human breast cancer in a brain metastatic model by G207, a replication-competent multimutated herpes simplex virus 1. Hum Gene Ther 1998;9(15): 2177–2185. [PubMed: 9794202]
32. Stiles BM, Bhargava A, Adusumilli PS, Stanziale SF, Kim TH, Rusch VW, et al. The replication-competent oncolytic herpes simplex mutant virus NV1066 is effective in the treatment of esophageal cancer. Surgery 2003;134(2):357–364. [PubMed: 12947341]
33. Stanziale SF, Stiles BM, Bhargava A, Kerns SA, Kalakonda N, Fong Y. Oncolytic herpes simplex virus-1 mutant expressing green fluorescent protein can detect and treat peritoneal cancer. Hum Gene Ther 2004;15(6):609–618. [PubMed: 15212719]
34. Nakamura H, Kasuya H, Mullen JT, Yoon SS, Pawlik TM, Chandrasekhar S, et al. Regulation of herpes simplex virus gamma(1)34.5 expression and oncolysis of diffuse liver metastases by Myb34.5. J Clin Invest 2002;109(7):871–882. [PubMed: 11927614]
35. Kooby DA, Carew JF, Halterman MW, Mack JE, Bertino JR, Blumgart LH, et al. Oncolytic viral therapy for human colorectal cancer and liver metastases using a multi-mutated herpes simplex virus type-1 (G207). FASEB J 1999;13(11):1325–1334. [PubMed: 10428757]
36. Ebright MI, Zager JS, Malhotra S, Delman KA, Weigel TL, Rusch VW, et al. Replication-competent herpes virus NV1020 as direct treatment of pleural cancer in a rat model. J Thorac Cardiovasc Surg 2002;124(1):123–129. [PubMed: 12091817]
37. Carew JF, Kooby DA, Halterman MW, Federoff HJ, Fong Y. Selective infection and cytolysis of human head and neck squamous cell carcinoma with sparing of normal mucosa by a cytotoxic herpes simplex virus type 1 (G207). Hum Gene Ther 1999;10(10):1599–1606. [PubMed: 10428205]
38. Varghese S, Rabkin SD. Oncolytic herpes simplex virus vectors for cancer virotherapy. Cancer Gene Ther 2002;9(12):967–978. [PubMed: 12522436]
39. Ebright MI, Zager JS, Malhotra S, Delman KA, Weigel TL, Rusch VW, et al. Replication-competent herpes virus NV1020 as direct treatment of pleural cancer in a rat model. J Thorac Cardiovasc Surg 2002;124(1):123–129. [PubMed: 12091817]
40. Sahn SA, Good JT Jr. Pleural fluid pH in malignant effusions. Diagnostic, prognostic, and therapeutic implications. Ann Intern Med 1988;108(3):345–349. [PubMed: 3341671]

41. Okumura M, Ohshima S, Kotake Y, Morino H, Kikui M, Yasumitsu T. Intraoperative pleural lavage cytology in lung cancer patients. Ann Thorac Surg 1991;51(4):599–604. [PubMed: 2012419]

42. Okada M, Tsubota N, Yoshimura M, Miyamoto Y, Maniwa Y. Role of pleural lavage cytology before resection for primary lung carcinoma. Ann Surg 1999;229(4):579–584. [PubMed: 10203093]

43. Kondo H, Asamura H, Suemasu K, Goya T, Tsuchiya R, Naruke T, et al. Prognostic significance of pleural lavage cytology immediately after thoracotomy in patients with lung cancer. J Thorac Cardiovasc Surg 1993;106(6):1092–1097. [PubMed: 8246544]

44. Kjellberg SI, Dresler CM, Goldberg M. Pleural cytologies in lung cancer without pleural effusions. Ann Thorac Surg 1997;64(4):941–944. [PubMed: 9354505]

45. Higashiyama M, Doi O, Kodama K, Yokouchi H, Tateishi R, Horai T, et al. Pleural lavage cytology immediately after thoracotomy and before closure of the thoracic cavity for lung cancer without pleural effusion and dissemination: clinicopathologic and prognostic analysis. Ann Surg Oncol 1997;4(5):409–415. [PubMed: 9259968]

46. Dresler CM, Fratelli C, Babb J. Prognostic value of positive pleural lavage in patients with lung cancer resection. Ann Thorac Surg 1999;67(5):1435–1439. [PubMed: 10355426]

47. Buhr J, Berghauser KH, Gonner S, Kelm C, Burkhardt EA, Padberg WM. The prognostic significance of tumor cell detection in intraoperative pleural lavage and lung tissue cultures for patients with lung cancer. J Thorac Cardiovasc Surg 1997;113(4):683–690. [PubMed: 9104977]

48. Johnston WW. The malignant pleural effusion. A review of cytopathologic diagnoses of 584 specimens from 472 consecutive patients. Cancer 1985;56(4):905–909. [PubMed: 4016683]

49. DiBonito L, Falconieri G, Colautti I, Bonifacio D, Dudine S. The positive pleural effusion. A retrospective study of cytopathologic diagnoses with autopsy confirmation. Acta Cytol 1992;36(3): 329–332. [PubMed: 1580116]

50. Chernow B, Sahn SA. Carcinomatous involvement of the pleura: an analysis of 96 patients. Am J Med 1977;63(5):695–702. [PubMed: 930945]

51. Ichinose Y, Tsuchiya R, Koike T, Yasumitsu T, Nakamura K, Tada H, et al. A prematurely terminated phase III trial of intraoperative intrapleural hypotonic cisplatin treatment in patients with resected non-small cell lung cancer with positive pleural lavage cytology: the incidence of carcinomatous pleuritis after surgical intervention. J Thorac Cardiovasc Surg 2002;123(4):695–699. [PubMed: 11986597]

52. Lerondel S, Le Pape A, Sene C, Faure L, Bernard S, Diot P, et al. Radioisotopic imaging allows optimization of adenovirus lung deposition for cystic fibrosis gene therapy. Hum Gene Ther 2001;12 (1):1–11. [PubMed: 11177537]

53. Jacobs A, Tjuvajev JG, Dubrovin M, Akhurst T, Balatoni J, Beattie B, et al. Positron emission tomography-based imaging of transgene expression mediated by replication-conditional, oncolytic herpes simplex virus type 1 mutant vectors in vivo. Cancer Res 2001;61(7):2983–2995. [PubMed: 11306477]

54. Hemminki A, Zinn KR, Liu B, Chaudhuri TR, Desmond RA, Rogers BE, et al. In vivo molecular chemotherapy and noninvasive imaging with an infectivity-enhanced adenovirus. J Natl Cancer Inst 2002;94(10):741–749. [PubMed: 12011224]

55. Bennett JJ, Tjuvajev J, Johnson P, Doubrovin M, Akhurst T, Malholtra S, et al. Positron emission tomography imaging for herpes virus infection: Implications for oncolytic viral treatments of cancer. Nat Med 2001;7(7):859–863. [PubMed: 11433353]

56. Jacobs A, Tjuvajev JG, Dubrovin M, Akhurst T, Balatoni J, Beattie B, et al. Positron emission tomography-based imaging of transgene expression mediated by replication-conditional, oncolytic herpes simplex virus type 1 mutant vectors in vivo. Cancer Res 2001;61(7):2983–2995. [PubMed: 11306477]

57. Groot-Wassink T, Aboagye EO, Glaser M, Lemoine NR, Vassaux G. Adenovirus biodistribution and noninvasive imaging of gene expression in vivo by positron emission tomography using human sodium/iodide symporter as reporter gene. Hum Gene Ther 2002;13(14):1723–1735. [PubMed: 12396625]

58. Bennett JJ, Tjuvajev J, Johnson P, Doubrovin M, Akhurst T, Malholtra S, et al. Positron emission tomography imaging for herpes virus infection: Implications for oncolytic viral treatments of cancer. Nat Med 2001;7(7):859–863. [PubMed: 11433353]

59. Haberkorn U, Altmann A. Functional genomics and radioisotope-based imaging procedures. Ann Med 2003;35(6):370–379. [PubMed: 14572160]
60. Yang M, Baranov E, Moossa AR, Penman S, Hoffman RM. Visualizing gene expression by whole-body fluorescence imaging. Proc Natl Acad Sci U S A 2000;97(22):12278–12282. [PubMed: 11050247]
61. Yang M, Baranov E, Jiang P, Sun FX, Li XM, Li L, et al. Whole-body optical imaging of green fluorescent protein-expressing tumors and metastases. Proc Natl Acad Sci U S A 2000;97(3):1206–1211. [PubMed: 10655509]
62. Tsutsudaasano A, Migita M, Takahashi K, Shimada T. Transduction of fibroblasts and CD34+ progenitors using a selectable retroviral vector containing cDNAs encoding arylsulfatase A and CD24. J Hum Genet 2000;45(1):18–23. [PubMed: 10697958]
63. Paquin A, Jaalouk DE, Galipeau J. Retrovector encoding a green fluorescent protein-herpes simplex virus thymidine kinase fusion protein serves as a versatile suicide/reporter for cell and gene therapy applications. Hum Gene Ther 2001;12(1):13–23. [PubMed: 11177538]
64. Mazurier F, Moreau-Gaudry F, Maguer-Satta V, Salesse S, Pigeonnier-Lagarde V, Ged C, et al. Rapid analysis and efficient selection of human transduced primitive hematopoietic cells using the humanized S65T green fluorescent protein. Gene Ther 1998;5(4):556–562. [PubMed: 9614582]
65. Jacobs A, Dubrovin M, Hewett J, Sena-Esteves M, Tan CW, Slack M, et al. Functional coexpression of HSV-1 thymidine kinase and green fluorescent protein: implications for noninvasive imaging of transgene expression. Neoplasia 1999;1(2):154–161. [PubMed: 10933050]
66. Hunt L, Jordan M, De Jesus M, Wurm FM. GFP-expressing mammalian cells for fast, sensitive, noninvasive cell growth assessment in a kinetic mode. Biotechnol Bioeng 1999;65(2):201–205. [PubMed: 10458741]
67. Prosst RL, Winkler S, Boehm E, Gahlen J. Thoracoscopic fluorescence diagnosis (TFD) of pleural malignancies: experimental studies. Thorax 2002;57(12):1005–1009. [PubMed: 12454292]
68. Gahlen J, Prosst RL, Pietschmann M, Rheinwald M, Haase T, Herfarth C. Spectrometry supports fluorescence staging laparoscopy after intraperitoneal aminolaevulinic acid lavage for gastrointestinal tumours. J Photochem Photobiol B 1999;52(1–3):131–135. [PubMed: 10643077]
69. Gahlen J, Stern J, Laubach HH, Pietschmann M, Herfarth C. Improving diagnostic staging laparoscopy using intraperitoneal lavage of delta-aminolevulinic acid (ALA) for laparoscopic fluorescence diagnosis. Surgery 1999;126(3):469–473. [PubMed: 10486597]
70. Gahlen J, Prosst RL, Pietschmann M, Haase T, Rheinwald M, Skopp G, et al. Laparoscopic fluorescence diagnosis for intraabdominal fluorescence targeting of peritoneal carcinosis experimental studies. Ann Surg 2002;235(2):252–260. [PubMed: 11807366]
71. Chishima T, Miyagi Y, Wang X, Yamaoka H, Shimada H, Moossa AR, et al. Cancer invasion and micrometastasis visualized in live tissue by green fluorescent protein expression. Cancer Res 1997;57(10):2042–2047. [PubMed: 9158003]
72. Hasegawa S, Yang M, Chishima T, Miyagi Y, Shimada H, Moossa AR, et al. In vivo tumor delivery of the green fluorescent protein gene to report future occurrence of metastasis. Cancer Gene Ther 2000;7(10):1336–1340. [PubMed: 11059691]
73. Chishima T, Miyagi Y, Wang X, Baranov E, Tan Y, Shimada H, et al. Metastatic patterns of lung cancer visualized live and in process by green fluorescence protein expression. Clin Exp Metastasis 1997;15(5):547–552. [PubMed: 9247257]
74. Chishima T, Miyagi Y, Wang X, Tan Y, Shimada H, Moossa A, et al. Visualization of the metastatic process by green fluorescent protein expression. Anticancer Res 1997;17(4A):2377–2384. [PubMed: 9252650]
75. Diehn FE, Costouros NG, Miller MS, Feldman AL, Alexander HR, Li KC, et al. Noninvasive fluorescent imaging reliably estimates biomass in vivo. Biotechniques 2002;33(6):1250–1255. [PubMed: 12503309]
76. Robinson PJ. Imaging liver metastases: current limitations and future prospects. Br J Radiol 2000;73(867):234–241. [PubMed: 10817037]
77. Hirsch FR, Franklin WA, Gazdar AF, Bunn PA Jr. Early detection of lung cancer: clinical perspectives of recent advances in biology and radiology. Clin Cancer Res 2001;7(1):5–22. [PubMed: 11205917]

78. Gahlen J, Prosst RL, Pietschmann M, Rheinwald M, Haase T, Herfarth C. Spectrometry supports fluorescence staging laparoscopy after intraperitoneal aminolaevulinic acid lavage for gastrointestinal tumours. J Photochem Photobiol B 1999;52(1–3):131–135. [PubMed: 10643077]

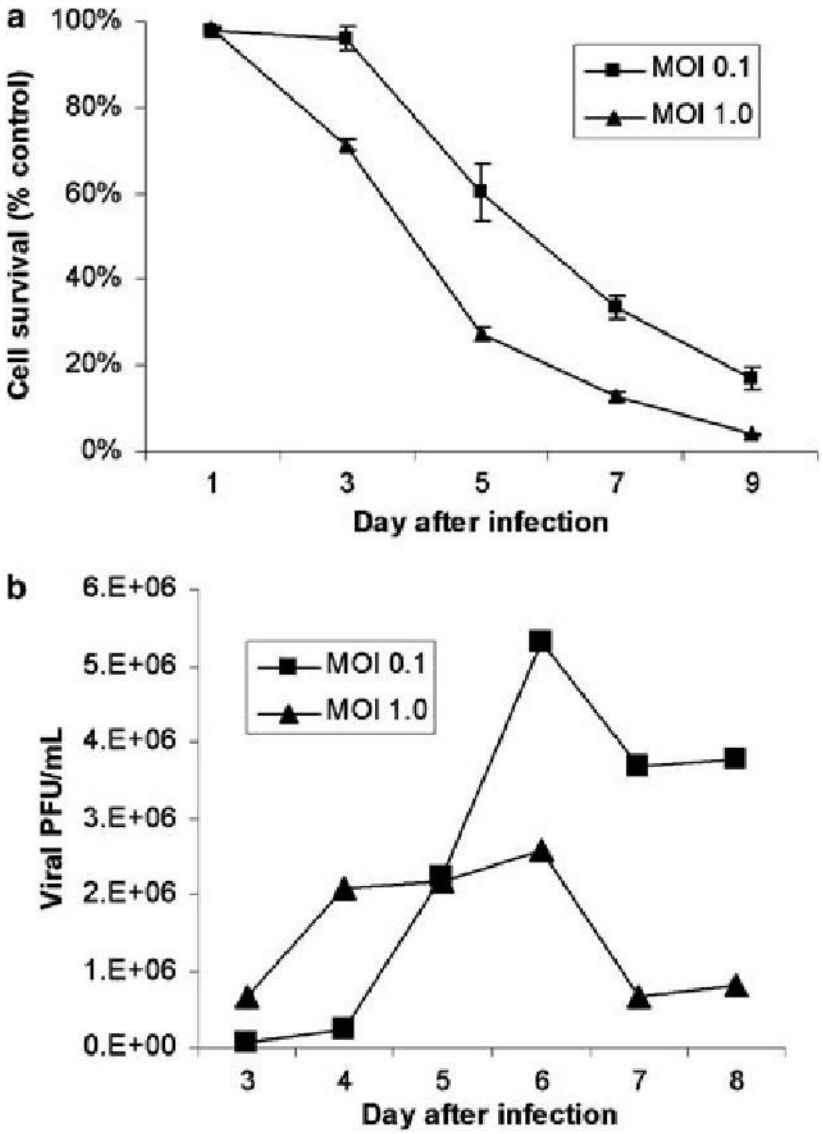

Figure 1.

(*A*) Cytotoxic effect of NV1066 on A549 cells. NV1066 effectively kills A549 cancer cells *in vitro* at multiplicities of infection (MOI) of 0.1 or 1.0. Results are expressed as cell survival compared to untreated control cells grown under identical conditions. (B) *In vitro* replication. NV1066 replicates in A549 cells, with peak viral titers demonstrating a 5300-fold increase over the original infecting dose of virus at an MOI of 0.1. Titers increased 260-fold at the higher MOI. Lower peak titers often occur with higher MOIs *in vitro*, as early cell death limits the time and cell number for productive viral replication.

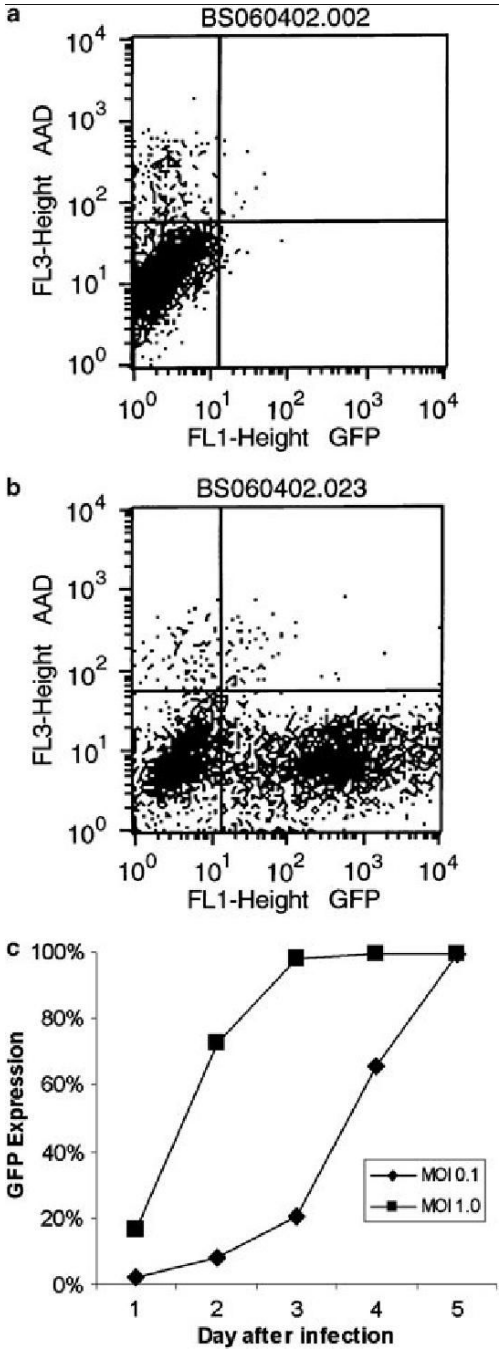

Figure 2.

EGFP expression. Following treatment with NV1066, infected A549 cells express EGFP, as determined by flow cytometry. The lower right hand quadrant of (*A*) and (*B*) represent live cells expressing EGFP. Control populations of cells did not express significant amounts of the reporter protein (*A*). Over 60% of cells infected with NV1066 at an MOI of 1.0 expressed EGFP after 48 hours (*B*). Represented as percent of live cells expressing EGFP over time (*C*), expression increased to nearly 100% with both MOIs after just five days, indicating that nearly all of the cells within the population were infected with NV1066.

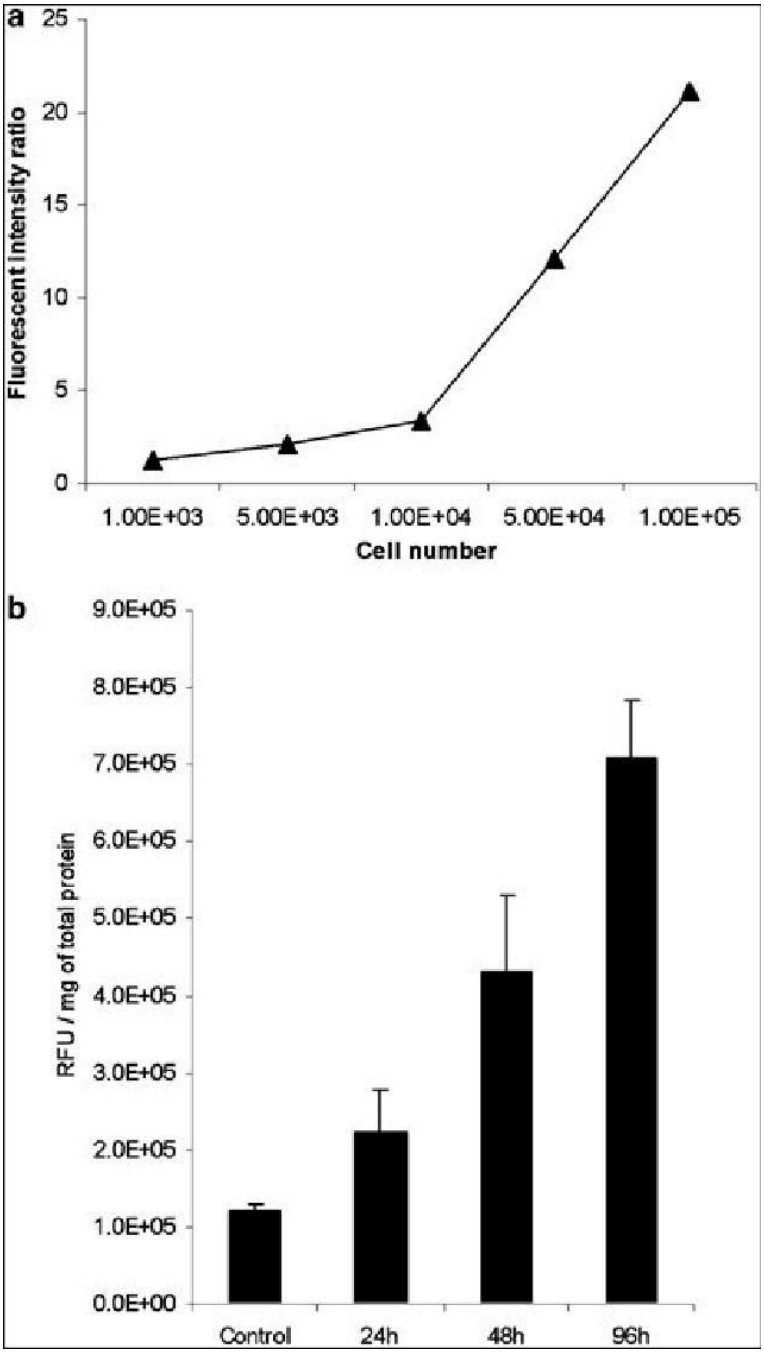

Figure 3.

Fluorimetry. The fluorescent signal from NV1066 infected cells increased linearly with cell number *in vitro* (*A*), suggesting that fluorescent intensity could be used as a surrogate for infected cell number. Fluorescent intensity ratios (fluorescence of infected cells/fluorescence of uninfected cells) reach sufficient levels to visually distinguish induced fluorescence from background fluorescence with as few as 1 x 10^4 cells infected with NV1066 *in vitro*. In *ex vivo* experiments, fluorescence increased over time in tumors infected with NV1066, representing viral replication and spread within the tumor (*B*). By 48 hours after infection, significant differences in the fluorescent signal were present between control and infected tumors ($p = .04$)

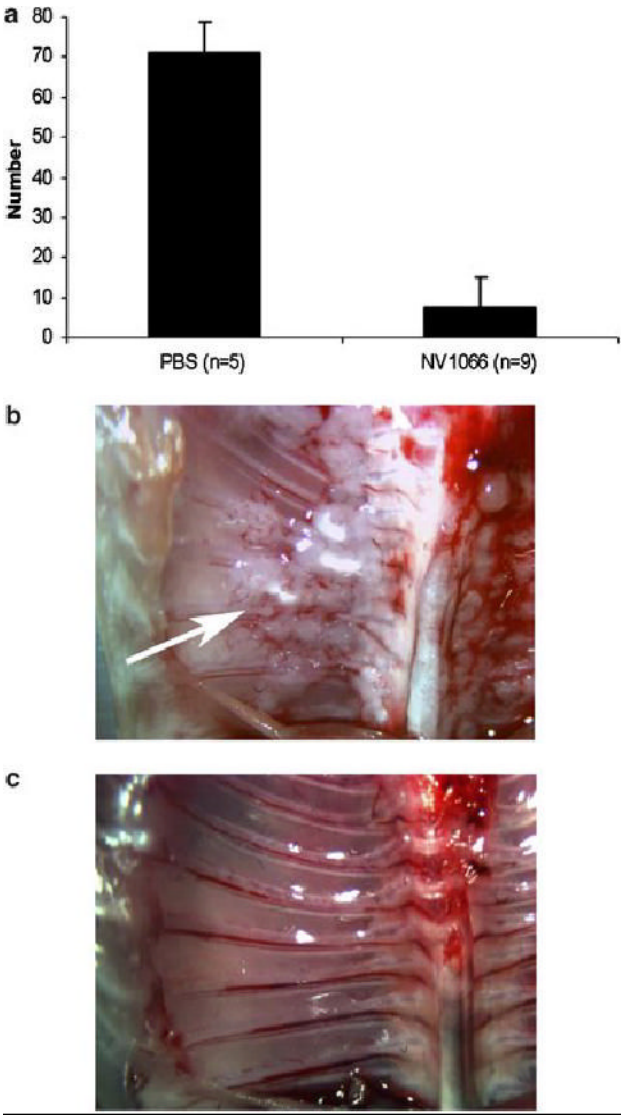

Figure 4.

Antitumor effect of NV1066 *in vivo*. In a metastatic tumor model, intrapleural injection of NV1066 decreased formation of chest wall tumor nodules, compared to treatment with PBS alone (*A*, $p < .001$) at 3 weeks. Representative photographs of the chest wall of a control mouse (*B*) and an NV1066-treated mouse (*C*) are shown (chest wall nodules shown with an arrow).

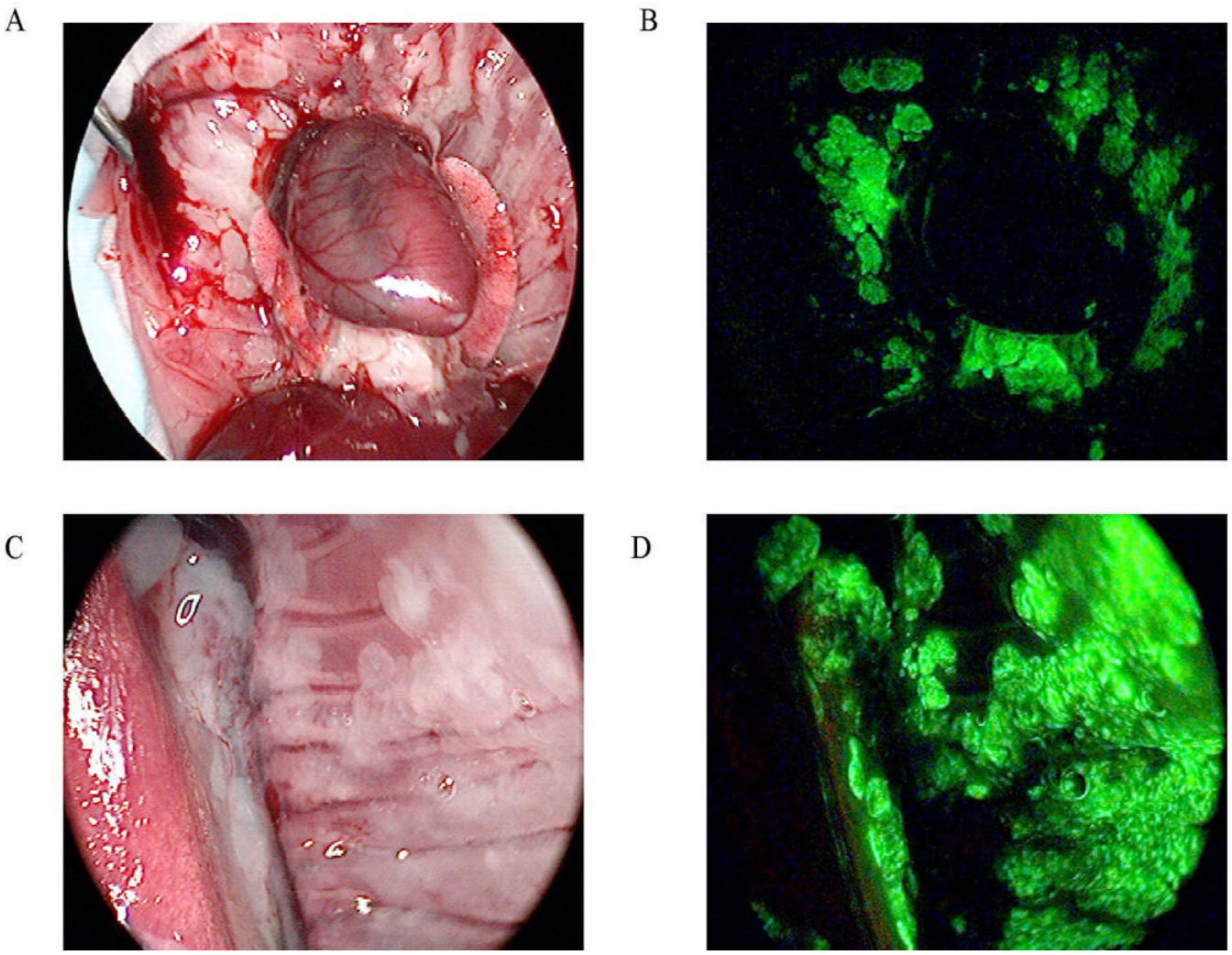

Figure 5.
In vivo EGFP expression following viral treatment. Using the fluorescent thoracoscopic system, the pleural cavities of mice with macroscopic tumor deposits were examined in white light (*A* and *C*) and GFP (*B* and *D*) modes. Following intrapleural treatment with NV1066 (48 hours), EGFP expression localized to tumor deposits, sparing normal tissues.

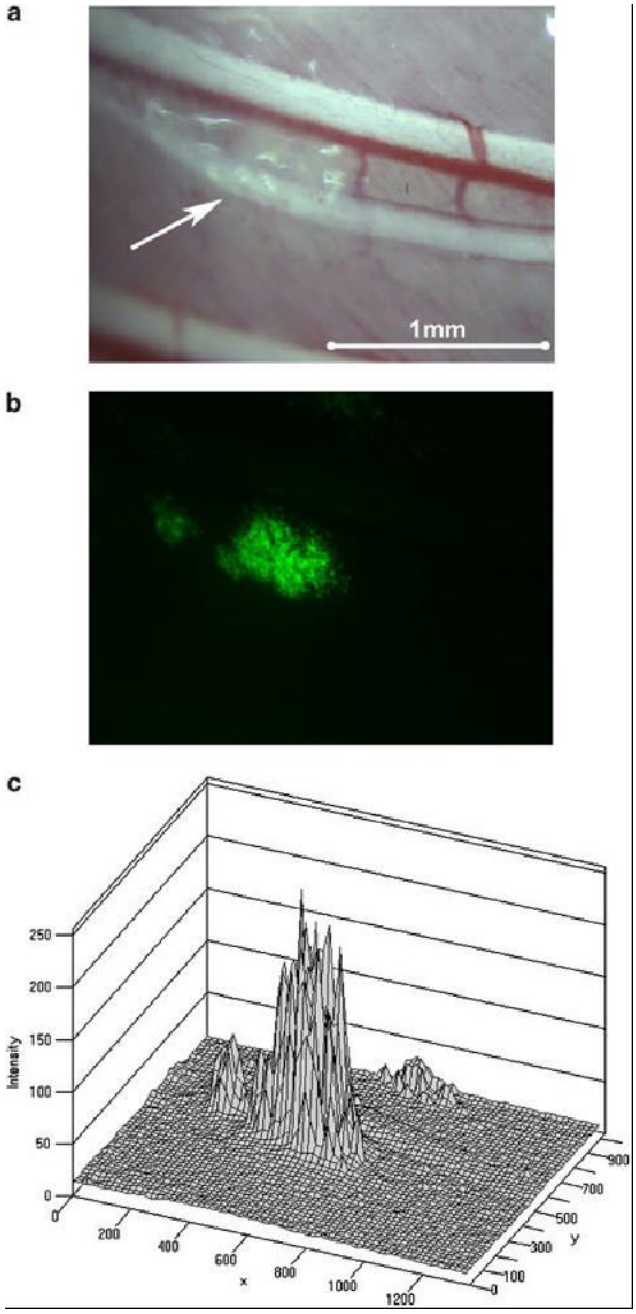

Figure 6.
Thoracoscopic identification of small metastatic tumor deposits. *In vivo* viral uptake and gene delivery could be detected in tumor deposits less than even a millimeter in size. Tumor deposits not clearly identified on white light thoracoscopy (*A, shown with an arrow*) could be identified by EGFP expression with fluorescent thoracoscopy (*B*). Topography maps of EGFP expression were digitally created to quantify fluorescent intensity relative to background (*C*).

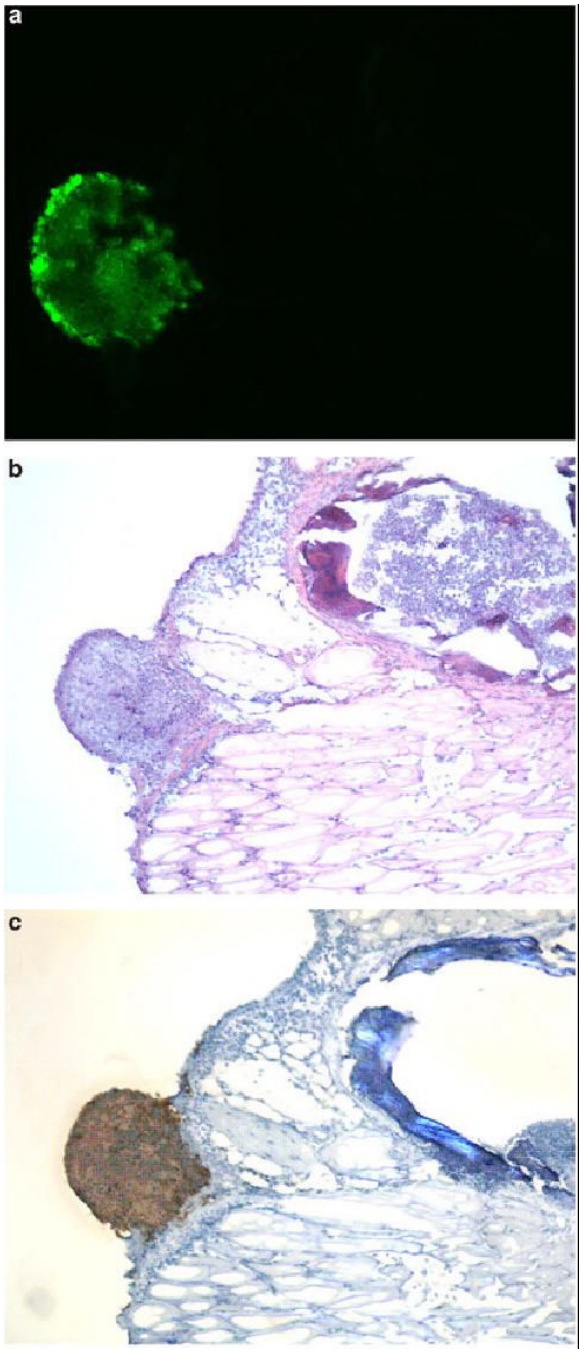

Figure 7.
Viral specificity for tumor. Tissue specimens were selected by EGFP expression under fluorescent stereomicroscopy in intact animals. Serial sectioning was performed and specimens were examined under fluorescent microscopy (*A*), then H & E stained (*B*) for identification of tumor cells. All sections that expressed EGFP had tumor cell infiltrates. Staining for polyclonal HSV-1 antibody corresponded to areas of EGFP expression and tumor (*C*). No viral staining was evident in tissues that did not express EGFP.